ISBN: 978-3-95450-234-9 ISSN: 2673-5504 doi:10.18429/JACoW-SRF2023-TUPTB020

SURFACE PROPERTIES AND RF PERFORMANCE OF VAPOR DIFFUSED Nb_3Sn ON NB AFTER SEQUENTIAL ANNEALS BELOW 1000 °C*

J. K. Tiskumara†, J. R. Delayen
Center for Accelerator Science, Old Dominion University, Norfolk, VA, USA
U. Pudasaini, Thomas Jefferson National Accelerator Facility, Newport News, VA, USA
G. Eremeev, Fermi National Accelerator Laboratory, Batavia, IL, USA

Abstract

Nb_3Sn is a next-generation superconducting material that can be used for future superconducting radiofrequency (SRF) accelerator cavities, promising better performance, cost reduction, and higher operating temperature than Nb. The Sn vapor diffusion method is currently the most preferred and successful technique to coat niobium cavities with Nb_3Sn. Among post-coating treatments to optimize the coating quality, higher temperature annealing without Sn is known to degrade Nb_3Sn because of Sn loss. We have investigated Nb_3Sn/Nb samples briefly annealed at 800-1000 °C for 10 and 20 minutes to potentially improve the surface to enhance the performance of Nb_3Sn-coated cavities. Following the sample studies, a coated single-cell cavity was sequentially annealed at 900 °C and tested its performance each time, improving the cavity's quality factor relatively. This paper summarizes the sample studies and discusses the RF test results from sequentially annealed SRF Nb_3Sn/Nb cavity.

INTRODUCTION

With a higher critical temperature $T_c \sim 18.3$ K and a superheating field $H_{sh} \sim 400$ mT (both twice that of Nb), Nb_3Sn is a potential alternative material to replace Nb in SRF cavities. Therefore, Nb_3Sn has the potential to exhibit lower dissipation compared to niobium at any given temperature due to its reduced surface resistance. Nb_3Sn cavities have demonstrated the ability to operate at 4 K while delivering performance similar to Nb cavities at 2 K. This offers a promising opportunity to reduce the operational cost of SRF accelerators. Furthermore, Nb_3Sn's superheating field indicates a higher breakdown field, enabling higher accelerating gradients and potentially reducing the initial cost of constructing SRF accelerators [1, 2]. However, Nb_3Sn is typically deposited as a thin film on already-built RF structures due to its brittleness and lower thermal conductivity. Among the various methods available, several laboratories have successfully pursued the Sn vapor diffusion technique to coat Nb SRF cavities with different shapes and frequencies. [3-7]. In this process, the Sn is evaporated and transported as a vapor to the substrate Nb at temperatures exceeding 930°C to form the Nb_3Sn phase. In Jefferson Lab, we have utilized the Nb_3Sn coating facility to coat various Nb cavities using the vapor diffusion technique. Most coatings have been grown on elliptical-shaped single-cell and multi-cell SRF cavities with a single beamline. Additionally, for the first time, we successfully coated and tested a twin-axis cavity with a complex geometry housing two beamlines [8]. This twin-axis cavity has been proposed for applications in Energy Recovery Linacs (ERL) [8].

After conducting the initial coating and RF testing on the twin-axis cavity, we encountered specific issues unique to this cavity coating and some common challenges observed in other cavity coatings. Among the major problems we identified were potential non-uniformity caused by hard-to-reach areas, the mechanical stability of the cavity after the high-temperature Nb_3Sn coating, and the surface quality of the deposited thin film. We noticed recurring roughness and Sn residues, similar to those in other cavity coatings. Previous studies have attempted various chemical treatments to enhance the surface quality of the coated surface [9], but an optimal process has yet to be developed.

In order to customize the coating process for the twin-axis cavity, we conducted extensive studies on different coating parameters. Based on these studies, we updated the coating parameters and implemented various treatments to improve the quality of the coated surface. This process included optimizing the Sn supply by reducing the amount of Sn used, adjusting the size of the crucible, and modifying the temperature profile to minimize the accumulation of Sn residues during and at the end of the coating process [1].

Sn residues on the coated surface posed a persistent challenge, but the updated coating parameters involved multi-step coating temperatures and gradual cooling below 900 °C helped reduce the size of Sn residues. One potential approach to mitigate Sn residues is to anneal the coated surface without Sn, thereby evaporating the remaining Sn residue. But with the Potential of Sn loss when annealed at temperatures higher than 1000 °C or lower temperatures for more than 45 minutes [1, 10], we limited our study to temperatures below 1000 °C (950 °C, 900 °C and 850 °C) for shorter time periods (10 and 20 minutes) which has not been studied earlier. In this paper, we will present the results from systematic studies conducted on Nb_3Sn samples that were annealed at temperatures below 1000 °C and the RF performance from sequentially annealed Nb_3Sn coated cavity.

* Research supported by DOE Office of Science Accelerator Stewardship Program Award DE-SC0019399 and DOE Award DE-SC0010081. Partially authored by Jefferson Science Associates under contract no. DEAC0506OR23177. This material is based upon work supported by the U.S. Department of Energy, Office of Science, Office of Nuclear Physics and Office of High Energy Physics .
† jtisk001@odu.edu

ISBN: 978-3-95450-234-9 ISSN: 2673-5504 doi:10.18429/JACoW-SRF2023-TUPTB020

EXPERIMENTAL

Sample Preparation and Nb_3Sn Coating

Similar high RRR, 3mm thick Nb sheets used to fabricate SRF cavities are used to make 10 mm × 10 mm samples. The samples underwent a process to remove the damaged layer from the surface, which involved applying 100 µm of Buffered Chemical Polishing (BCP). Subsequently, they were subjected to a heat treatment at 800 °C for 3 hours to facilitate hydrogen degassing. Finally, a 5 µm BCP removal was performed on the samples before the deposition of Nb_3Sn coating [1].

The samples for this study were coated using a similar coating process used to coat single-cell cavities recently at JLab, which includes the temperature profile of 1 hour of nucleation at 500 °C followed by about 3 h of coating (~ 40 min at 1200 °C, 45 min at 1150 °C, and 85 min 1100 °C). Following the coating, the temperature was ramped down at 1 °C/min to 800 °C before the heater turned off, similar to the twin axis cavity coating. Samples were coated inside a Nb chamber using 0.9 g of Sn loaded into a 0.5" diameter crucible and 0.5 g of $SnCl_2$ packaged inside Nb foil [1, 2, 10]. Each sample was coated uniformly with expected Sn residues similar to the twin axis cavity coating [1].

Annealing experiments

The coated samples were annealed at 850 ± 5 °C, 900 ± 5 °C and 950 ± 5 °C for 10 min and 20 min. After annealing, the samples were subjected to various characterization techniques to investigate the effects of the annealing process on composition, microstructure, topography, and surface features. Special attention was given to the size and distribution of Sn residue. In the following section, we will delve into the results of the material studies conducted on the annealed samples.

MATERIAL STUDIES

The coated and annealed samples were examined using Atomic Force Microscopy (AFM), Scanning Electron Microscopy (SEM) equipped with Energy Dispersive Spectroscopy (EDS) detectors, and X-Ray Diffraction (XRD).

AFM

The topography of each sample was analyzed with a Digital Instruments Nanoscope IV AFM in tapping mode. Samples were scanned at 3 randomly chosen locations with 5 µm × 5 µm, 10 µm × 10 µm, 20 µm × 20 µm, and 50 µm × 50 µm scan sizes.

As expected, the coated samples displayed a consistent and even distribution of Sn residue, as depicted in the top left figure of both Figs. 1 and 2. Notably, the annealed samples did not exhibit any features similar to those observed in samples annealed at temperatures higher than 975 °C in previous experiments [1, 10]. The Sn residues varied in size, ranging from a few nanometers to several tens of nanometers. The height of numerous Sn residues was measured for each sample, and the average height is summarized in Table 1. It is evident that both the density and height of Sn residue were reduced after the annealing process, with a more pronounced effect observed at higher annealing temperatures.

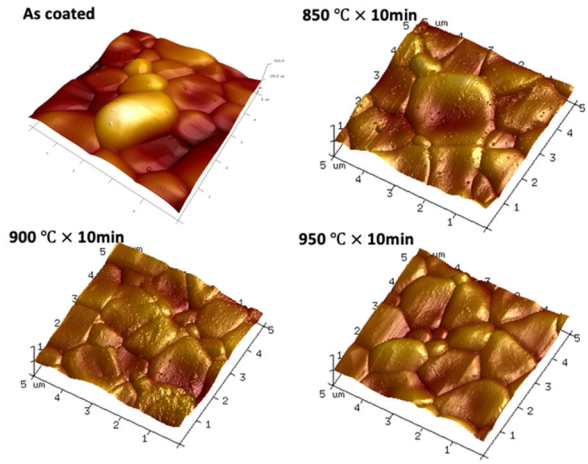

Figure 1: AFM images of the as coated and annealed samples for 10 minutes at different temperatures.

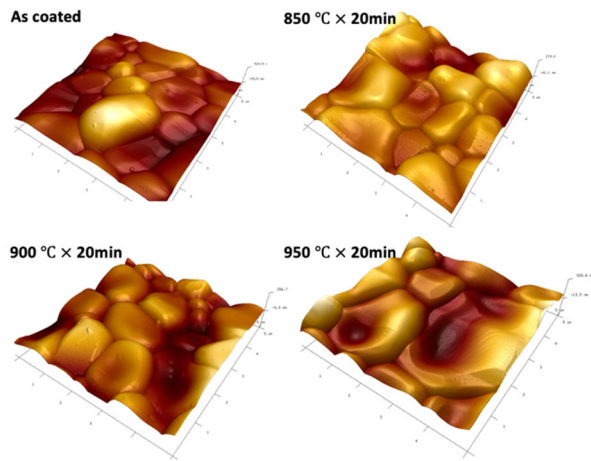

Figure 2: AFM images of the as coated and annealed samples for 20 minutes at different temperatures.

Table 1: Average Height of the Sn Residue

	Average height of the Sn residue (nm)
As coated	10.7 ± 3.1
850 °C × 10 min	10.1 ± 2.2
900 °C × 10 min	6.8 ± 0.8
950 °C × 10 min	5.2 ± 1.5
850 °C × 20 min	5.1 ± 2.4
900 °C × 20 min	4.6 ± 2.4
950 °C × 20 min	2.8 ± 1.8

ISBN: 978-3-95450-234-9 ISSN: 2673-5504 doi:10.18429/JACoW-SRF2023-TUPTB020

SEM

The elemental composition of each sample was analyzed by energy dispersive x-ray spectrometry (EDS) with Hitachi 4700 field emission scanning electron microscope (FE-SEM) or Phenom ProX.

SEM was used to examine the microstructure of as-coated and annealed samples. SEM images were used to estimate the grain size and analyze Sn particles on the surface. The representative SEM images from each coated and annealed sample are shown in Figs. 3 and 4. Note that nanoscopic Sn residue is not visible in this magnification. The estimated average grain size for each sample is presented in Table 2.

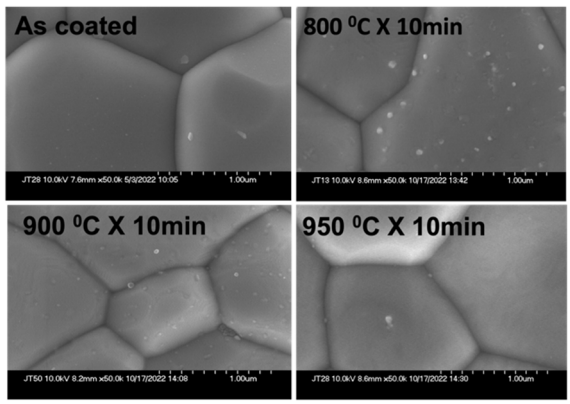

Figure 3: SEM images of the as coated and annealed samples for 10 minutes at different temperatures.

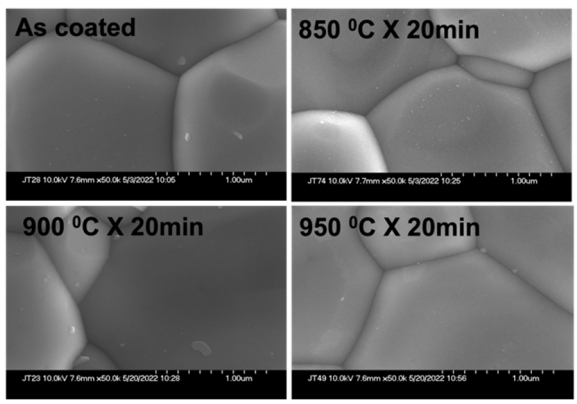

Figure 4: SEM images of the as coated and annealed samples for 20 minutes at different temperatures.

Surprisingly, there was no observable correlation between the annealing temperature or time and the grain size. The variation in grain size fell within the error bar, indicating that the annealing time at lower temperatures was insufficient to induce any significant changes in grain size.

EDS measurements were conducted at least three locations within each sample to assess the elemental composition and then averaged. However, no significant changes in the Sn content within the coating were observed after the annealing process, regardless of the annealing profile studied. These findings are presented in Table 2. It is worth noting that while these values were averaged over several locations, they do not suggest any noticeable accumulation of Sn at the grain boundaries [11].

Table 2: Average Grain Size and the Sn Composition of the Samples SEM Images of the As-coated and Annealed Samples for 10 and 20 Minutes at Different Temperatures

	Average grain size (μm)	Average Sn %
As coated	1.23 ± 0.01	24.90 ± 0.56
850 °C × 10 min	1.37 ± 0.03	24.83 ± 0.16
900 °C× 10 min	1.26 ± 0.08	24.89 ± 0.15
950 °C× 10 min	1.36 ± 0.03	24.78 ± 0.17
850 °C × 20 min	1.26 ± 0.05	24.93 ± 0.22
900 °C× 20 min	1.19 ± 0.07	25.07 ± 0.28
950 °C× 20 min	1.21 ± 0.10	24.98 ± 0.11

XRD

X-Ray Diffraction (XRD) pattern of the coating before and after annealing were obtained from Rigaku Miniflex II X-ray diffractometer with Cu-α radiation.

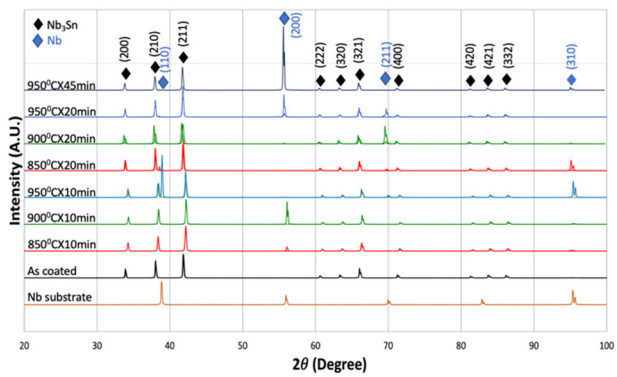

Figure 5: XRD peaks of the samples.

The X-ray diffraction (XRD) analysis presented in the above Fig. 5 shows the peaks obtained from a Nb sample (substrate), the as-coated sample, and the annealed samples (as well as samples annealed at 950 °C for 45 minutes which gave annealing features). As expected, only Nb_3Sn peaks were observed in the as-coated sample, confirming the Nb_3Sn phase. Interestingly, the Nb_3Sn phase demonstrated stability in terms of grain orientation across all annealing temperatures. However, on several annealed samples, new peaks emerged, primarily corresponding to the Nb substrate. Note the strong Nb peaks in the samples annealed at 950 °C may suggest the possibility of Sn loss from the shallow surface of the Nb_3Sn layers. This observation aligns with the annealing features observed in the

ISBN: 978-3-95450-234-9 ISSN: 2673-5504 doi:10.18429/JACoW-SRF2023-TUPTB020

Atomic Force Microscopy (AFM) and Scanning Electron Microscopy (SEM) images, resembling those observed at higher annealing temperatures. Nonetheless, it is important to consider that the Nb peaks could also be associated with the Nb substrate, as the annealing process may have resulted in thinning of the Nb_3Sn layer at specific locations. The data may suggest Sn loss at higher temperatures or longer annealing [11].

ANNEALING A CAVITY AND RF TEST RESULTS

Single Cell Cavity Annealing

Following interesting and promising sample study results, we wanted to use it in an actual Nb_3Sn coated SRF cavity to investigate the effect of annealing on RF performance. This TE1NS001 single cell cavity is coated following the same optimized procedure as we coated the samples and the twin axis cavity. First, we annealed the coated cavity for 10 minutes at 900 °C and RF tested. We selected 900 °C as the annealing temperature as 950 °C had resulted in annealing features, and other phases of Nb-Sn are possible around 850 °C. We ramped up to 500 °C first, parked there for 30 minutes, and then to 900 °C for 10 minutes. Later, after the RF testing, it is annealed for another 10 minutes to complete the annealing time of 20 minutes.

RF Performances.

After the annealing for 10 minutes at 900 °C, the cavity is high pressure rinsed, assembled in the clean room, and forwarded to the RF testing at cryogenic temperatures.

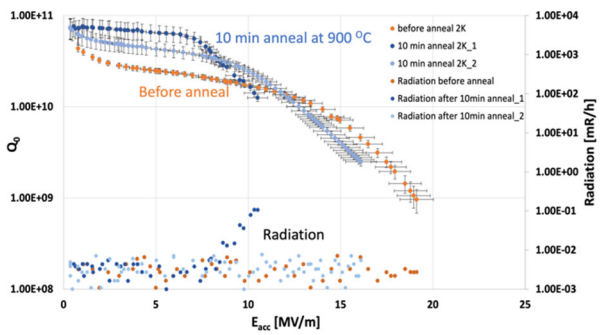

Figure 6: SEM images of the as coated and annealed samples for 20 minutes at different temperatures.

As shown in Fig. 6, the quality factor of the annealed cavity started to decrease exponentially above 7 MV/m. With the observed field emission, followed another additional high-pressure water rinse with ultra-pure water and retested. In the re-test the cavity reached a higher accelerating gradient to about 16 MV/m and cavity gradient was limited by quench. The enhancement observed in the low field quality factor of the cavity after annealing indicates that the surface quality of the film has improved as a result of the annealing process. Our hypothesis for observed low-field quality factor improvement contributed by two factors. Firstly, the reduction in volume of Sn residue leads to a decrease in the suppression of superconductivity caused by the proximity effect. Secondly, the reduction in the height of Sn islands contributes to improving surface roughness. These conclusions are supported by our investigations on small samples [11].

Following the RF test, the cavity was annealed for another 10 minutes to evaluate the afftect of 20 minutes of annealing.

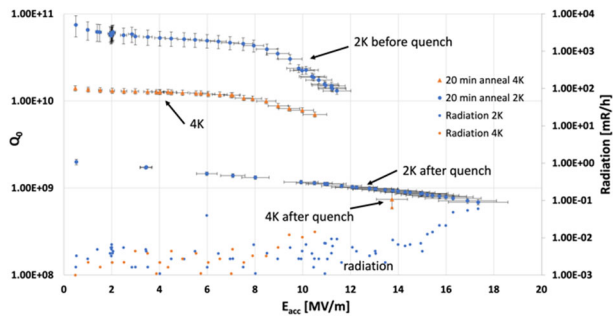

Figure 7: SEM images of the as coated and annealed samples for 20 minutes at different temperatures.

According to Fig. 7, the cavity experienced quenching at around 10.5 MV/m at 4 K, which improved to approximately 11.5 MV/m at 2 K. However, the quality factor of the cavity decreased after the quench at both temperatures. Additionally, we observed signs of multipacting. The low field quality factor was comparable to that obtained after a 10-minute annealing process. Despite the decrease in the quality factor following the quench, we achieved an acceleration gradient of approximately 17 MV/m, limited by the RF power available.

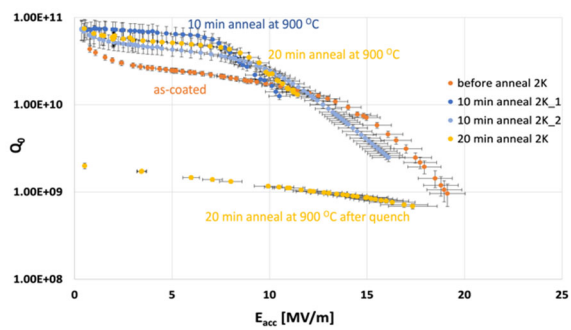

Figure 8: SEM images of the as coated and annealed samples for 20 minutes at different temperatures.

Figure 8 summarizes the RF results of both annealing conditions. In both 10 and 20 minutes of annealing, the low field Q is increased with the Sn residue height reduction. However, it is worth noting that the high-field Q-factor may not always exhibit improvement after annealing. This improvement is due to the potential formation of Sn-enriched regions at grain boundaries during the annealing process. These regions can act as pinning centers for magnetic flux vortices, reducing the high-field Q-factor [11].

ISBN: 978-3-95450-234-9 ISSN: 2673-5504 doi:10.18429/JACoW-SRF2023-TUPTB020

SUMMARY AND OUTLOOK

The condensation of Sn residue limits the performance of Nb_3Sn cavities. A sample study was conducted to investigate the impact of low-temperature annealing on surface Sn residue and microstructure in Nb_3Sn coatings. Higher temperature annealing processes result in Sn loss from the Nb_3Sn coating, leading to film quality degradation. Therefore, we annealed samples at temperatures of 850 °C, 900 °C, and 950 °C for durations of 10 and 20 minutes and subsequently analyzed the samples with various material characterization tools.

Upon analysis, it was observed that the height of the Sn residues decreases with increasing annealing temperature. However, no clear trend was observed regarding grain size, Sn composition, or surface roughness as the annealing temperature increased. Notably, X-ray diffraction (XRD) analysis revealed the appearance of Nb peaks for samples annealed, potentially suggesting Sn loss from the shallow surface or thinning of coating layers following the annealing.

Annealing resulted in changes in the performance of the of Nb_3Sn coated cavity. The low-field Q-factor is improved by reducing the surface defects and, thus, the surface resistance. The high-field Q-factor may not improve with the annealing as Sn enriches grain boundaries, and the heating of residues with increasing RF power may potentially occur. These low temperatures annealing results highlighted the potential benefits of annealing in improving the performance of Nb_3Sn cavities, but further studies are needed.

ACKNOWLEDGEMENT

We are grateful for the JLab staff who helped us with this research. We thank Applied Research Center Core Labs at the College of William & Mary for allowing us to use the SEM and AFM instruments. We are grateful to Olga Trofimova for helping with the AFM analysis. Thanks to M. S. Shakel from Old Dominion University for the help with XRD measurements.

REFERENCES

[1] J. K. Tiskumara, J. R. Delayen, G. V. Eremeev, and U. Pudasaini, "Lower Temperature Annealing of Vapor Diffused Nb_3Sn for Accelerator Cavities", in *Proc. NAPAC'22*, Albuquerque, NM, USA, Aug. 2022, pp. 695-698. doi:10.18429/JACoW-NAPAC2022-WEPA31

[2] J. K. Tiskumara, J. R. Delayen, G. V. Eremeev, U. Pudasaini, and C. E. Reece, "Nb3Sn Coating of Twin Axis Cavity for SRF Applications", in *Proc. SRF'21*, East Lansing, MI, USA, Jun.-Jul. 2021, pp. 146. doi:10.18429/JACoW-SRF2021-SUPTEV011

[3] U. Pudasaini *et al.*, "Nb3Sn Multicell Cavity Coating at JLab", in *Proc. IPAC'18*, Vancouver, Canada, Apr.-May 2018, pp. 1798-1803. doi:10.18429/JACoW-IPAC2018-WEYGBF3

[4] S. Posen *et al.*, "Development of Nb3Sn Coatings for Superconducting RF Cavities at Fermilab", in *Proc. IPAC'18*, Vancouver, Canada, Apr.-May 2018, pp. 2718-2720. doi:10.18429/JACoW-IPAC2018-WEPML016

[5] S. Posen *et al.*, "Development of Nb3Sn Coatings for Superconducting RF Cavities at Fermilab", in *Proc. IPAC'18*, Vancouver, Canada, Apr.-May 2018, pp. 2718-2720. doi:10.18429/JACoW-IPAC2018-WEPML016

[6] K. Takahashi *et al.*, "First Nb3Sn Coating and Cavity Performance Result at KEK", in *Proc. SRF'21*, East Lansing, MI, USA, Jun.-Jul. 2021, pp. 27. doi:10.18429/JACoW-SRF2021-SUPCAV009

[7] Z. Q. Yang *et al.*, "Development of Nb3Sn Cavity Coating at IMP", in *Proc. SRF'19*, Dresden, Germany, Jun.-Jul. 2019, pp. 21-24. doi:10.18429/JACoW-SRF2019-MOP003

[8] J. K. Tiskumara *et al.*, "Nb3Sn Coating of Twin Axis Cavity for Accelerator Applications", in *Proc. IPAC'21*, Campinas, Brazil, May 2021, pp. 1175-1178. doi:10.18429/JACoW-IPAC2021-MOPAB384

[9] S. Posen, "Understanding and Overcoming Limitation Mechanism in Nb3Sn superconducting RF Cavities," Ph.D. thesis, Cornell University, USA, 2015.

[10] U. Pudasaini, C. E. Reece, and J. K. Tiskumara, "Managing Sn-Supply to Tune Surface Characteristics of Vapor-Diffusion Coating of Nb3Sn", in *Proc. SRF'21*, East Lansing, MI, USA, Jun.-Jul. 2021, pp. 516. doi:10.18429/JACoW-SRF2021-TUPTEV013

[11] J. K. Tiskumara, "Nb3Sn Coating of Twin Axis Cavity and Other Complex SRF Cavity Structures", Ph.D thesis, Old Dominion University, USA, 2023.